Analyst

Interdisciplinary detection science

www.rsc.org/analyst

Volume 136 | Number 8 | 21 April 2011 | Pages 1525–1768

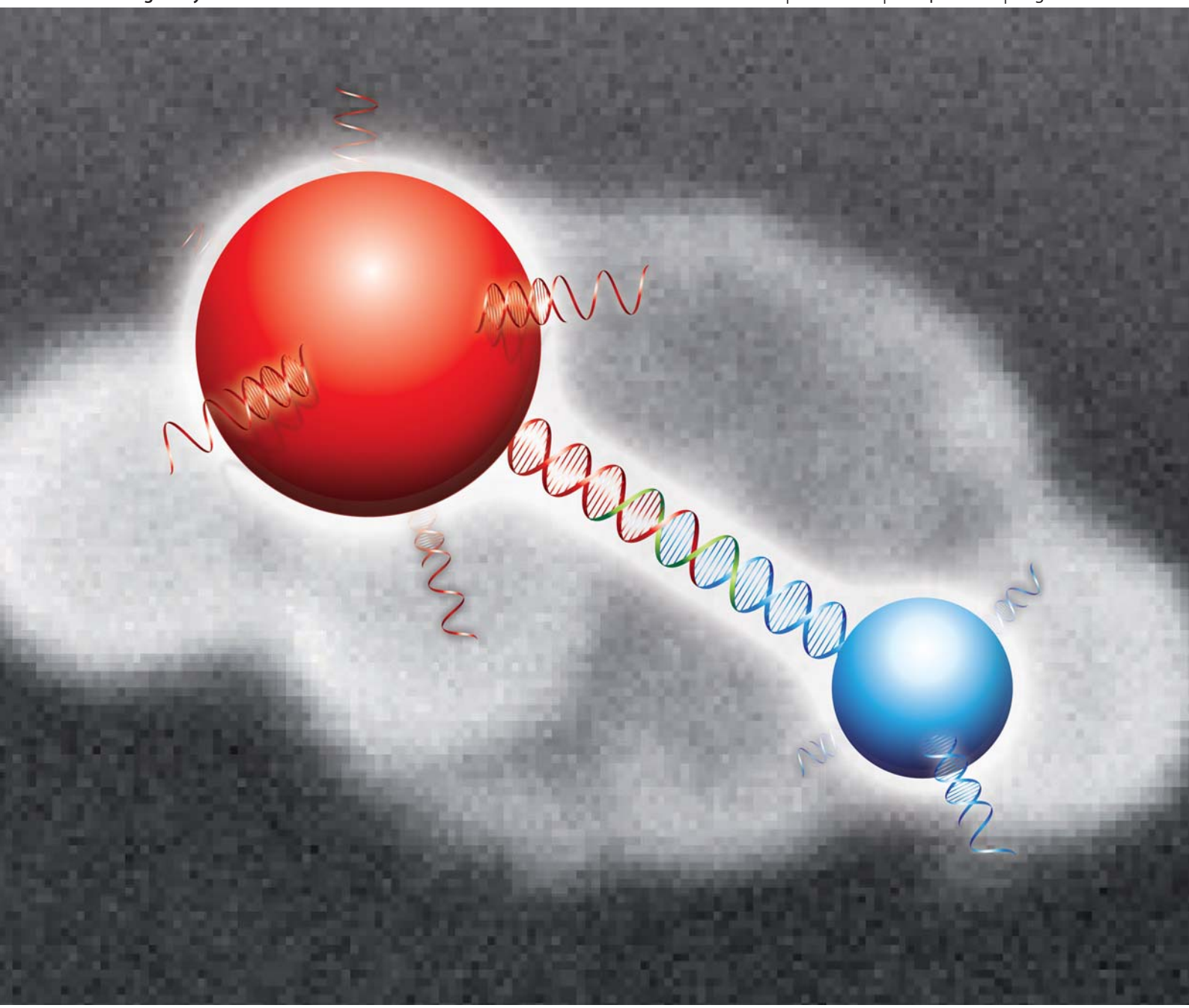

ISSN 0003-2654

RSC Publishing

HOT ARTICLE

Matthew A. Cooper *et al.*

Amplification free detection of Herpes Simplex Virus DNA

Analyst

Dynamic Article Links

Cite this: *Analyst*, 2011, **136**, 1599

www.rsc.org/analyst

PAPER

Amplification free detection of Herpes Simplex Virus DNA†

David A. C. Thomson,[ab] Krassen Dimitrov[a] and Matthew A. Cooper*[b]

Received 20th December 2010, Accepted 8th February 2011
DOI: 10.1039/c0an01021a

Amplification-free detection of nucleic acids in complex biological samples is an important technology for clinical diagnostics, especially in the case where the detection is quantitative and highly sensitive. Here we present the detection of a synthetic DNA sequence from Herpes Simplex Virus-1 within swine cerebrospinal fluid (CSF), using a sandwich-like, magnetic nanoparticle pull-down assay. Magnetic nanoparticles and fluorescent polystyrene nanoparticles were both modified with DNA probes, able to hybridise either end of the target DNA, forming the sandwich-like complex which can be captured magnetically and detected by fluorescence. The concentration of the target DNA was determined by counting individual and aggregated fluorescent nanoparticles on a planar glass surface within a fluidic chamber. DNA probe coupling for both nanoparticles was optimized. Polystyrene reporter nanoparticles that had been modified with amine terminated DNA probes were also treated with amine terminated polyethylene glycol, in order to reduce non-specific aggregation and target independent adhesion to the magnetic particles. This way, a limit of detection for the target DNA of 0.8 pM and 1 pM could be achieved for hybridisation buffer and CSF respectively, corresponding to 0.072 and 0.090 femtomoles of target DNA, in a volume of 0.090 mL.

Introduction

The *Herpesviridae* are a large family of DNA viruses, whose members can cause several diseases including oral and genital herpes, chicken pox, shingles, glandular fever and congenital cytomegalovirus disease. The infections are typically characterised by a long-term latency, which on reactivation, are able to cause significant morbidity and mortality, especially in patients with compromised immune systems, such as organ transplant recipients and HIV infected individuals. In addition, infection of the central nervous system and sensory organs by members of these Herpes viruses can cause severe outcomes for patients.[1] Encephalitis caused by Herpes Simplex Virus (HSV) is the most common non-seasonal encephalitis and occurs in an estimated 2.2 people per million, per year.[2] Patients with suspected Herpes Simplex Encephalitis (HSE), are usually immediately prescribed with antiviral drugs, as the mortality rate in untreated patients can be as high as 70%.[3]

Detection of Herpes Simplex Virus (HSV) in human cerebrospinal fluid (CSF) was one of the first clinical applications of Polymerase Chain Reaction (PCR).[3,4] This and other nucleic acid amplification methods were shown to be superior to serological or viral cultural analysis techniques, as they offered a more accurate indication of viral infection or reactivation. Serology can be problematic as antibody titre can be diminished in immune-compromised patients[5] and may lead to the risk of false negative results. However, target amplification methods also have their limitations, even though they possess excellent sensitivity[6] and specificity. Their limitations are: (a) the risk of false positives arising from contamination during sample preparation, (b) requirement for implementation of temperature-controlled instrumentation, and (c) the risk of false negatives due to sample contamination with PCR inhibitors. Furthermore, many of the PCR based tests for HSV are custom protocols which exhibit considerable variability from one laboratory to another, complicating inter-laboratory comparison.[7]

In contrast to target amplification, signal amplification involves techniques in which a label is bound directly to the target molecule, creating a signal sufficiently strong that it can be resolved against a system background. Many nanoparticle based detection systems have been developed for nucleic acid assays, for instance (a) DNA functionalised gold colloid which exhibits colour changes upon target induced aggregation,[8] (b) oligonucleotide functionalised gold as in the DNA-bar-code assay,[9] (c) nanoparticles with time-resolvable fluorescence properties[10] and (d) electrochemically detected nanoparticle labels.[11] These labels are typically analysed by either a digital single particle method[12] or by an analogous approach determining the net aggregate signal. The sensitivities for these assays range across many logs of dynamic range with the highest performance effectively approaching single molecule sensitivity (Table 1).

[a]*Institute for Molecular Biosciences, University of Queensland, Brisbane, Australia. E-mail: m.cooper@uq.edu.au*
[b]*Australian Institute for Bioengineering and Nanotechnology, University of Queensland, Brisbane, Australia*

† Electronic supplementary information (ESI) available: Mathematical expressions used to calculate the number of particles, flow cytometry data. See DOI: 10.1039/c0an01021a

Table 1 Comparison of sensitivity for various amplification free nucleic acid hybridisation assays

Assay format	Detection	Sensitivity	Ref
Target dependent aggregation of gold nanoparticles	Evanescent wave induced scattering with colour change indicating target presence	3.3×10^{-19}	8
Target capture on magnetic beads followed by binding dual labelled gold nanoparticles	DNA barcode detection on solid phase using silver precipitation on gold nanoparticles enhanced optical scattering	5.0×10^{-19}	9
Magnetic bead capture of target DNA molecules followed by probe binding	Europium (III) nanoparticle label with time resolved fluorescence	1.0×10^{-18}	10
Target capture followed by magnetic extraction and labelling with latex particles	Counting of magnetically pulled down 850 nm latex particles	1.7×10^{-18}	15
Target capture and magnetic extraction followed by nanoparticle labelling	Enhanced chemiluminescence with AuNP–luminol–$AgNO_3$	6.0×10^{-17}	16
Magnetic bead capture and extraction (current work)	Fluorescent nanoparticle and aggregate counting	7.2×10^{-17}	
Solid phase capture with target displacement by oligolabelled nanoparticles	Signal generated by stripping voltammetry of metal sulfide nanoparticle label	1.0×10^{-16}	11

One key differentiator among these techniques is whether target capture and its detection are conducted on a solid support, similar to a microarray format, or in solution phase. Solid support formats enable extensive multiplexing but are limited by long capture incubation times, in order to compensate limited mass-transport by diffusion. These limitations can be overcome by using particles, and especially nanoparticles with their enhanced surface area and faster diffusion rates.

The methodology reported here comprises a monoplex nanoparticle assay in which DNA capture probes immobilised on 500 nm magnetic nanoparticles are hybridised with the target DNA, in this case synthetic target DNA sequences derived from HSV. The hybridisation with the magnetic nanoparticles was followed by a second hybridisation with a reporter DNA probe coupled to fluorescently labelled polystyrene 200 nm particles (Fig. 1). The resulting sandwich structure, consisting of magnetic and fluorescent nanoparticles linked by target DNA, was magnetically extracted and then washed to remove unbound fluorescent particles. A direct counting method was developed, utilising microfluidic chambers and confocal fluorescence microscopy, which enables the quantitative analysis of the target DNA concentration (Fig. 2). Coupling methods and buffer components were first optimised using an aggregate fluorescence intensity method before detection using the microfluidics chambers, first in a buffer and then in the cerebrospinal fluid.

Materials and methods

Probe and target sequences

Virus specific DNA sequences for HSV were adapted from the genes quantitatively amplified by Stocher *et al.*[13] The probe length was extended by flanking sequences of the virus genome to obtain a 37 basepair target sequence with complementary capture and reporter probes (Table 2). The sequences were analyzed with IDT SciTools Oligoanalyzer[14] to determine the secondary structure of hairpins and homodimers. All nucleic acids used in the study were purchased from Integrated DNA Technologies (Coralville, USA).

Fluorescent nanoparticle probe coupling

Reporter DNA probe coupling studies were conducted to determine optimal concentration of DNA probe in the coupling

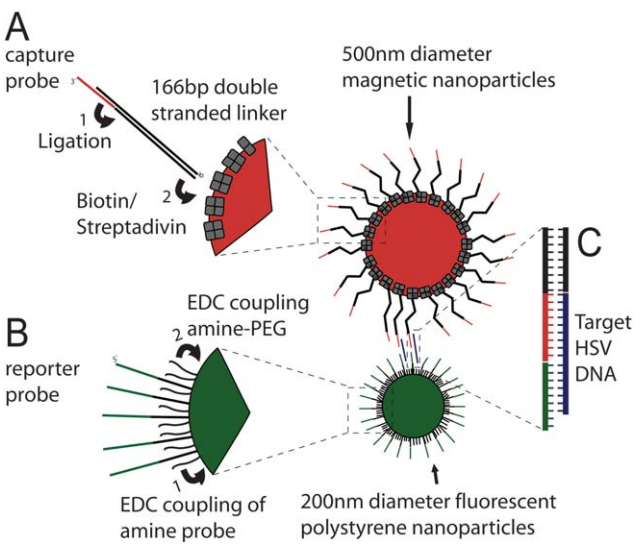

Fig. 1 Schematic of nanoparticle functionalization with HSV specific capture and reporter probes. (A) Phosphorylated capture probes were first ligated with 166 basepair biotinylated DNA molecules and then subsequently immobilized onto 500 nm streptadivin coated magnetic beads (red). (B) Amine labeled reporter probes were coupled to 200 nm fluorescent polystyrene nanoparticles (green) using EDC as a coupling agent. Subsequently, amine terminated polyethylene glycol molecules were coupled to the bead surface to reduce non-specific particle interactions. (C) Target HSV DNA linked to the magnetic and fluorescent particles resulting in a DNA dependent dose response.

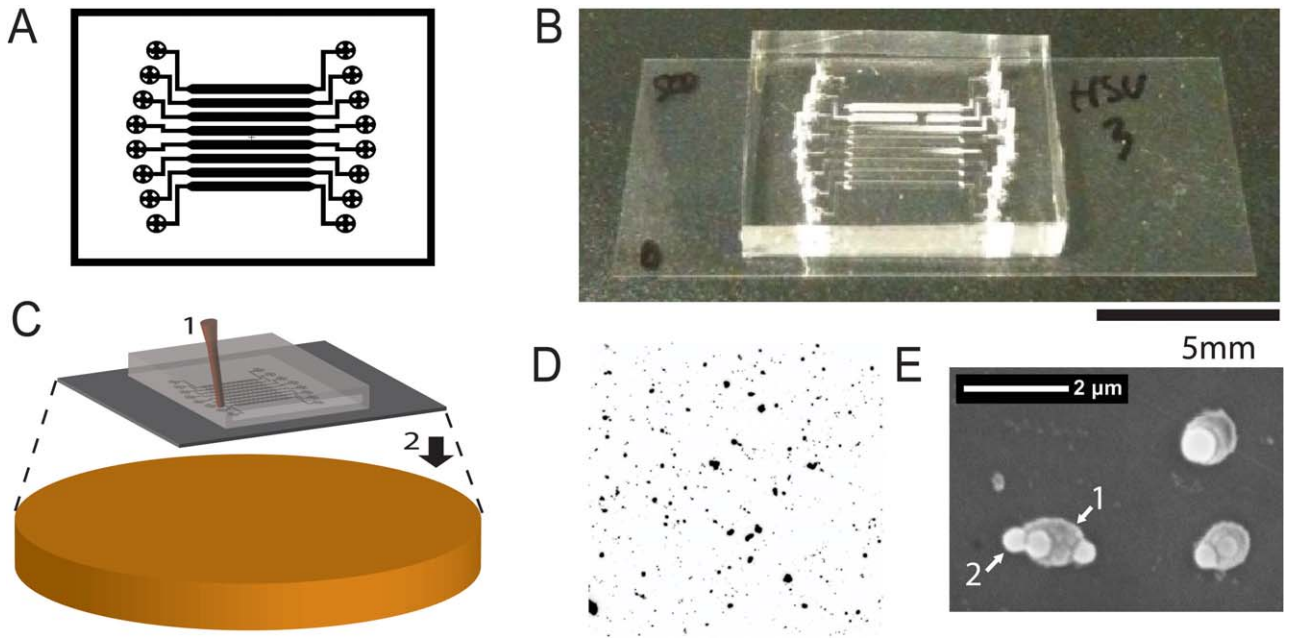

Fig. 2 (A) Design of mesoscale chamber device, developed in polydimethylsiloxane, and used for particle and aggregate counting on a confocal fluorescence microscope. (B) Photograph of realized device (scale bar refers to both A and B). (C) The device was first manually filled with a pipette and then placed on a 50 mm diameter disk magnet before being imaged. (D) Image of particles and aggregates obtained from hybridisation reaction with 50 pM target DNA. (E) Scanning Electron Microscopy image of structures formed at the limit of detection showing 500 nm magnetic beads (1) and 200 nm polystyrene nanoparticles (2).

reaction using 1-ethyl-3-(3-dimethylaminopropyl) carbodiimide (EDC). Yellow-Green 200 nm, carboxylic acid functionalised polystyrene fluospheres (Invitrogen, F8811, LOT759339; 4.5×10^{12} mL^{-1}) were washed three times into 60 mM 2-(*N*-morpholino)ethanesulfonic acid (MES Buffer), pH 5.5 with a Quantum Scientific Sigma Centrifuge at 14 000 rpm for 15 min before being resuspended into 100 µL at 1.1×10^{12} pr mL^{-1}. Particles were sonicated for 1 min after the final resuspension. The loading of the DNA probe was tested by adding amine terminated HSVp2 reporter probes, at three different concentrations: 6.0×10^{12}, 8.0×10^{12}, 1.0×10^{13} and 1.2×10^{13} probes per cm^2. A second 8.0×10^{12} probes per cm^2 reaction was prepared for the comparison of coupling *O*-(2-aminoethyl)-*O*′-methylpolyethylene glycol (Sigma, 07964-250MG, hereafter referred to as amine-PEG) to the particle surface. Freshly prepared 1-ethyl-3-(3-dimethylaminopropyl) carbodiimide (EDC) was added to the coupling reaction to a final concentration of 5 mM.[17] After 45 mins, another 500 nanomoles of EDC was added with particles incubated on a roller shaker for 105 min in darkness.

The amine-PEG was coupled onto the fluospheres for 30 minutes at 3×10^6 molar excess to nanoparticles equivalent to a concentration of 5.7 mM. Finally, any remaining carboxylic acid groups were capped with ethanolamine for 30 min at 100 mM. The particles were then washed four times in 0.4× SSC (60 mM NaCl, 6 mM trisodium citrate), 0.1% Triton X-100 pH 8, with final resuspension to give 7.3×10^{10} particles per mL (pr mL^{-1}). Batch couplings were conducted with 300 µL of fluosphere stock using identical incubation times and concentrations with 10^{13} probes per cm^2 as the coupling density and with amine-PEG treatment.

Magnetic nanoparticle probe coupling

Streptadivin coated 500 nm diameter Masterbeads from Adem-tech (Pessac, France, ~6.4×10^{10} particles per mL) were used throughout the study (StreptaDivin is neutralized form of avidin without carbohydrates and tripeptide sequence Arg–Tyr–Asp (RYD), these features provide for very low non-specific binding). The particles were coupled to a 166 basepair (bp) double stranded DNA linker with a single stranded capture probe (HSVp1) ligated to its terminus. Ligation of the capture probe before or after coupling the linker to the particle was compared. This was followed by the determination of optimum double stranded linker to magnetic bead biotin binding capacity. The double stranded linker was first hybridised using equimolar quantities of the single stranded ultramers, Ultra_DT_002 and Ultra_DT_004 (Table 2) in 200 µL of 300 mM NaCl, 30 mM trisodium citrate (pH 8), heating to 95 °C and passively cooling within a heat block over 120 min. Linker loading titrations were conducted at 0.6, 0.8, 1 and 1.2 molar excess of the biotinylated oligonucleotide binding capacity (2.4×10^{12} biotins per cm^2) of the particles for both on and off bead ligation. The linker coupling was performed in 5× SSC, 0.1% Triton X-100 (750 mM NaCl, 75 mM trisodium citrate, pH 8) for 180 min on a roller.

For the on-bead ligation, particles were washed three times into T4 DNA Ligase Buffer (50 mM Tris–HCl, 10 mM $MgCl_2$, 1 mM ATP, 10 mM dithiothreitol, pH 7.5, New England Biosciences). The HSVp1 capture probe was added at 10 molar equivalents to the linker and ligated with 0.5 µL of 400 000 per mL cohesive end units of T4 DNA ligase (NEB) at room temperature, on a roller shaker for 180 min. Off-bead ligation

Table 2 Target, capture and reporter probe sequences for Herpes Simplex Virus

DNA molecule	Sequence
HSVTar	NC_00186; 65605-65569[a] (UL30 DNA Polymerase Gene) CAG CTT GGT GAA CGT CTT TTC GCA CTC GAG TTT GAT G, M_w 11 377.4, Max Hairpin −0.95 kcal mol^{-1}, Max Self Dimer −12.64 kcal mol^{-} $^{-1}$
HSVp1	/5Phos/CTG ATC TCC CTC GTT GGC GCC ATC AAA CTC GAG TGC GAA (55C), M_w 11 983.7, Max Hairpin −2.24 kcal mol^{-1}, Max Self Dimer −19.94 kcal mol^{-1}
HSVp2	AAG ACG TTC ACC AAG CTG AAA AAA AAA AAA AAA/ 3AmMO/(54C), M_w 10 401.9, Max Hairpin −0.2 kcal mol^{-1}, Max Self Dimer −6.34 kcal mol^{-1}
Ultra_DT_002	/5Biosg/CGT CCC GCT TCA AAT ACG CCA CGT ATA GGT CTA TCA CGA TAC TCT CTG AAG TTG CCT AGG ATT GAC AGT CAG GTC CGC GGG AGT TTA CGC TTT TAT ATG TCT ACC GAC GAA GTA TTT CGC ACA CCG CTC CGG TAG AGA CCT GTC TT, M_w 45 257.4
Ultra_DT_004	GCG CCA ACG AGG GAG ATC AGA AGA CAG GTC TCT ACC GGA GCG GTG TGC GAA ATA CTT CGT CGG TAG ACA TAT AAA AGC GTA AAC TCC CGC GGA CCT GAC TGT CAA TCC TAG GCA ACT TCA GAG AGT ATC GTG ATA GAC CTA TAC GTG GCG TAT TTG AAG CGG GAC G, M_w 51 488
HSVTar-iCy5	CAG CTT GGT GAA CGT CTT/ iCy5/TTC GCA CTC GAGTTT GAT G (M_w 44 864.1)
CMV Tar (HHV5)	NC_006273.2; 121510-121546, TGG GAC ACA ACA CCG TAA AGC CGT TGC GCT CGT GGG G

[a] Accession number and position of target sequence in virus genome.

was conducted for 120 min with 10× molar excess of HSVp1 to the linker with 0.5 μL of T4 DNA ligase in 50 μL of DNA ligase buffer. The product of the ligation reaction was added directly to the magnetic beads for coupling *via* the biotin. Following ligation and coupling the beads were washed with 0.4× SSC, 0.1% Triton X-100, pH 8. It was assumed that 20% of the particles were lost in the linking process. Particles were stored ready-for-use at a concentration of ~10^9 pr mL^{-1}.

Batch couplings were conducted with 1.2 times molar excess of linker to biotin binding capacity with ligation conducted prior to coupling to the particle surface with 10 molar equivalents of capture probe HSVp1.

Capture and reporter probe density

Estimation of the capture and reporter DNA probe density was made on batch couplings for the magnetic and fluorescent nanoparticles using a flow cytometry saturation method. Cy5 labelled target DNA (HSVTar-iCy5) was hybridised to a fixed number of particles (1×10^9 fluospheres, 9.56×10^7 magnetic beads) in a 180 min incubation (4× SSC, 0.1% Triton X-100, pH 7.9). A series of reactions were conducted with increasing quantities of fluorescent target with a range of 0 to 3200 femtomoles. The geometric mean of the fluorescence intensity (Red laser, 660/20 filter) of each bead as measured on a BD FACSCantoII was plotted to determine the fluorescent saturation quantity. The resultant data are presented in the ESI† yielding estimates for probes per particles of 2760/magnetic bead and 753/fluorescent particle with a surface coverage of 3.5×10^{11} probes per cm^2 and 6.0×10^{11} probes per cm^2 for the magnetic and fluorescent particles, respectively.

Hybridisation assays

Hybridisation assays were conducted on a Biotek PrecisionXS robotic system using BD Falcon™ assay plate storage 96 well V-bottom polypropylene 96 well plates (cat. 353263). All bead and particle optimisation assays were conducted in a two step manner where the target DNA was first bound to magnetic beads (10^7) in a 90 μL reaction, for 90 min, with robotic pipetting every five minutes to mix the samples and keep the particles suspended. 10 μL of fluorescent reporter particles (7.26×10^8) was subsequently added, followed by another 90 minute hybridisation with robotic mixing every 5 minutes. Reactions were conducted, unless otherwise stated, in 4× SSC (600 mM NaCl, 60 mM trisodium citrate, 0.1% Triton X-100, pH 8, 25 μg mL^{-1} single stranded calf thymus DNA (Sigma D8899-5 mg)). Following hybridisation, the particles were washed with five cycles of magnetic capture on a 96 position magnet rack (Agencourt Bioscience Corporation, AGN #32782 SPRIplate) and resuspended into a final volume of 80 μL post-hybridisation buffer (0.4× SSC (60 mM, 6 mM trisodium citrate, 0.1% Triton X-100, pH 8, 25 μg mL^{-1} calf thymus DNA) for aggregate plate reading analysis or 20 μL for injection into the microfluidic chamber. The buffer ionic strength experiment was conducted in 4×, 2.67×, 1.33×, 0.67×, 0.33×, 0.17× SSC in 0.1% Triton X-100 with washing conducted in 0.4× SSC 0.1% Triton X-100. The target DNA was typically serially diluted for final reaction concentrations of 500, 50, 5, 0.5, 0.05 pM and zero target control.

Surfactant selection was performed using 2 mM concentration of Tween20, Triton X-100, *n*-dodecyl-β-D-maltoside (DDM), cetyl trimethylammonium bromide (CTAB) and 3-[(3-cholamidopropyl)dimethylammonio]-1-propanesulfonate (CHAPS) with 4× SSC for the hybridisation reaction. Post-hybridisation wash steps were conducted in 0.4× SSC (60 mM NaCl, 6 mM trisodium citrate, pH 8).

Microplate aggregate fluorescence assays

Aggregate fluorescent measurements were made on a BMG Labtech PolarSTAR Omega with a 485 nm/10 nm excitation filter and 510 nm/10 nm emission filter. Samples were loaded into

Black 96-well Microtest polystyrene assay plate from BD (353241) for aggregate measurements.

PDMS device fabrication

The devices used to define a fixed volume of particles were designed in L-EDIT (Tanner Research, USA) and fabricated using standard SU8 and PDMS processing.[18] Each device had eight chambers (5 × 1 mm) with a pitch of 1.125 mm and height of ~0.2 mm. SU8-2100 (Microchem, USA) was used to make the mould for PDMS fabrication. Photoresist was spun (1; 15 s, 500 rpm, 133 rpm s^{-1}, 2; 45 s, 1500 rpm, 400 rpm s^{-1}) and soft baked (1; 65 °C, 6 minutes, 2; 95 °C 20 minutes). The wafer was then exposed through a photomask printed on a HY2 high precision photoplate (Konica-Minolta, Japan), with 314 mJ cm^{-2} using an OAI blanket exposure system. The mask was printed with a high resolution Mivatec photoplotter (MIVA Technologies GmbH, Germany). Post exposure, wafers were baked for 5 min at 65 °C and 12 min at 95 °C and then developed in propylene glycol monoethyl ether acetate (PGMEA) until features were fully resolved. Sylgard 184 was mixed with cross-linker 10% w/w, vacuum degassed and poured over the mould and heated at 65 °C for 120 min. Devices were manually diced with fluid inlet and outlet holes punched prior to placing the device onto a glass cover slip for injection. Devices were washed for reuse in running water with gentle manual agitation.

Particle and aggregate counting

Particle and aggregate counting was conducted on an inverted laser scanning confocal microscope (Carl Zeiss, LSM710). Each chamber with the PDMS device was injected with particles and then placed on a high disk magnet (AussieMagnets, #3243; 50.8 mm diameter and 12.7 mm height) for 30 seconds. Particles were imaged with the pinhole set at 3.0 Airy Units using a 20 × 0.4 numerical aperture objective lens with particles excited at 5% laser power from a 488 nm laser with emission collected between 510 nm and 530 nm. The multi-time-series automation macro was utilised to image within each chamber and each of the eight chambers within a device. Images were processed with ImageJ,[19] counting objects greater than 4 square pixels.

CSF collection

Swine cerebrospinal fluid was collected from the lumbar region of a sacrificed animal at the Herston Medical Research Centre, Brisbane. The sample was placed immediately on dry ice and frozen at −20 °C. When used, samples were defrosted and DNA was spiked and serially diluted to create the dose response. Ethics approval for CSF collection was obtained (see notes).

Results and discussion

Before the assay was conducted in the microfluidic chambers, the reaction conditions for capture and reporter DNA coupling to the nanoparticles were optimized. This optimization was done by variation of buffer conditions, including ionic strength and surfactant concentrations, and selecting conditions for efficient hybridisation and minimum background. The assay was then conducted in the microfluidic chambers, to further optimize the volume analysis and methods.

Reporter probe coupling to fluorescent nanoparticles

One of the key factors to achieve a high sensitivity and a linear dose response, is the concentration of the DNA probe on the nanoparticle. Hybridisation efficiency is influenced by the surface probe density,[20] which for flat surfaces is typically in the range of 10^{12}–10^{13} probes per cm^2.[21] With increasing probe surface density, target diffusion and entry decreases, mainly due to electrostatic repulsion and steric hindrances, thereby decreasing the hybridisation efficiency.[20,22] With this in mind it was important to optimise the probe concentrations in the coupling reactions. Carboxylic acid functionalized polystyrene particles, similar to those utilised in this report, were first coupled with single stranded DNA by Kremsky and Wolf in 1987,[23,24] with a number of subsequent reports appearing in both the diagnostic[25] and the DNA self-assembly literature.[26–29]

In this study the coupling agent 1-ethyl-3-(3-dimethylaminopropyl) carbodiimide (EDC) was used to conjugate amine-terminated oligonucleotide probes to the carboxylic acid functionalised polystyrene fluorescent nanoparticles. The optimisation of the coupling reaction was developed with a range of probe concentrations corresponding to 6×10^{12}, 8×10^{12}, 1×10^{13} and 1.2×10^{13} probes per cm^2 of particle surface area. This was conducted in low salt concentration, to minimise particle aggregation, and at moderately low pH of 5.5, to prolong the lifetime of the EDC coupling reagent. The supplier of the nanoparticle reports 0.1–2 milliequivalents (millimoles per gram) of carboxylic acid per gram of particles, which corresponds to 2.2×10^{-19}–4.4×10^{-18} moles of acid per bead or 1.1×10^{14} and 2.1×10^{15} acid groups per cm^2. For the coupling reaction we used 1.1×10^{11} particles, corresponding to 25–500 nanomoles of carboxylic acid. For the coupling reaction we also used a 5 mM EDC solution corresponding thereby to a molar excess of 1–20.

The effect of different coupling probe concentrations on the hybridisation reaction was assayed. The target DNA was first hybridised with 10^7 capture probe coated magnetic beads with 500 pM and zero DNA in a 90 μL reaction. Reporter probe coupled fluospheres were added and, following a 90 minute hybridisation and 5 wash steps, the particles were assayed in a fluorescent plate reader. A probe to surface area of 10^{13} probes per cm^2 gave the optimum signal to background compared with the three other probe concentrations as shown in Fig. 3. This concentration was taken forward for subsequent batch probe yellow-green fluosphere conjugations. The specificity of the assay was also investigated by using a non-specific DNA molecule derived from the genome for cytomegalovirus (Table 2). Aggregate fluorescent data (Fig. 3) show no significant difference between 500 pM and no DNA controls.

In any sensitive biomolecule assay the importance of inhibiting non-specific interactions cannot be overstated. This is true for signal amplification techniques and in particular when using hydrophobic polystyrene nanoparticle labels, which have a tendency to give a high background.[29,30] Although these particles are functionalized with carboxylic acid groups and coupled with oligonucleotides, the fluospheres retain some level of surface hydrophobicity and therefore can non-specifically

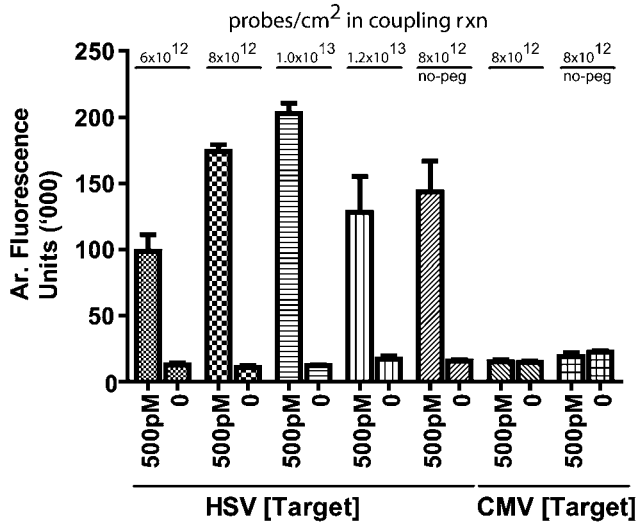

Fig. 3 Ratios of reporter probes to total surface area of polystyrene nanoparticles used to determine optimal coupling conditions for the assay. Nanoparticles were added to hybridisation reactions with 10^7 magnetic beads with either 500 pM or zero DNA. After automated washing aggregate fluorescent measurements were taken and graphed. Optimum result was achieved for 10^{13} probes per cm^2 with amine PEG co-modification. Cytomegalovirus DNA was added to two hybridisation reactions to assess specificity and effect of adding amine PEG to the coupling reaction. Both reactions produced low signals with PEG treatment aiding in reducing non-specific interactions ($n = 3$, error bars are standard error of mean).

bind the magnetic particles leading to background signal. Empirically, magnetically mobile fluorescent particles were observable in control hybridisation experiments in the absence of target DNA. These were inherently indistinguishable from reporter particles bound specifically with target DNA and define one aspect of the limit of detection for the assay.

To further improve the assay a number of surfactants were evaluated to reduce undesired non-specific interactions with the magnetic beads. The underlying rationale was to coat the uncharged surface of the nanoparticle with a surfactant. This could confer a neutral, cationic or anionic polar character of the surfactant to the particle. The microscope counting technique was used to determine the zero target background for 5 different detergents (Fig. 4). The non-ionic surfactant *n*-dodecyl-β-D-maltoside (DDM) has been reported to inhibit protein binding to polydimethylsiloxane[31] and so was tested to inhibit fluosphere binding to the magnetic particles. Interestingly, DDM gave the lowest counts in a zero target control hybridisation. However, a poor dose response was observed (data not shown), and so Triton X-100 was chosen as the optimal surfactant.

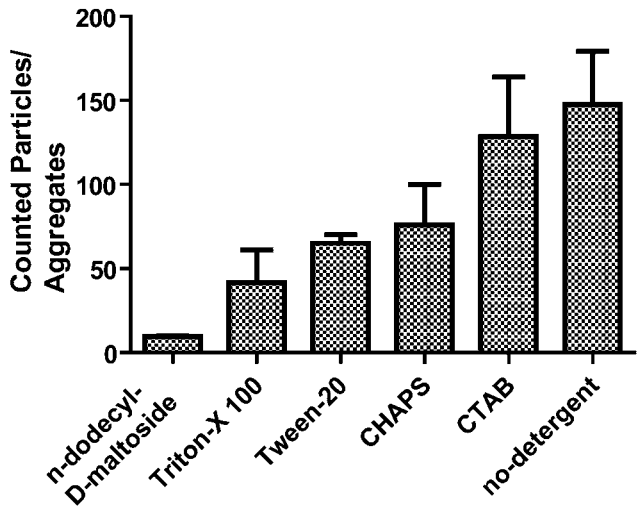

Fig. 4 Surfactants tested to reduce non-specific binding for the assay. Particles and aggregates were counted from hybridisation reactions with zero target DNA ($n = 3$, error bars are standard error of mean).

In addition to using surfactants to reduce non-specific interactions, the covalent attachment of a 750 Dalton methoxypolyethylene glycol amine to the surface of the polystyrene particles was investigated. Polyethylene glycol is widely used as a linker in hetero and homo bi-functional crosslinkers as a method of increasing the hydrophilicity of biomolecules.[32] Many reports have used PEG as an inhibitor of non-specific binding,[33–36] with many theoretical studies conducted elucidating variables such as chain length and density as important in reducing protein adhesion.[37] The ideal surface for inhibiting aggregation and non-specific binding is a densely packed monolayer with a consistent and well defined length.[34] In addition, the capture probe should extend out beyond the randomly coiled ethylene oxide polymer to enable the desired biomolecular interaction. The polymer used in this study was analysed using mass spectrometry which showed polydispersity ranging from 11 to 19 monomer ethylene glycol units.

Latex particles similar to those used in the current work have been previously modified to impart low binding and enable colloidal stability. For example, polyethylene oxide and polypropylene oxide or poly(diethyleneglycol ethylether acrylate)-polyacrylic acid diblock polymers have been coupled to beads to create surfaces compatible with colloidal crystal formation.[29] Another polymeric nanoparticle modification method uses solvent swelling, where hydrophobic portions of diblock polymers are trapped upon volatile solvent evaporation.[38] While elegant, this method would likely be problematic for dye embedded particles as the dye would leach out during the swelling step modification.

In the current work an amine PEG with an average of 14 monomer repeats was covalently coupled to the bead surface, using the same EDC coupling chemistry following probe immobilisation. In order to determine its effectiveness in reducing non-specific binding, an experiment was conducted in which the non-complementary DNA derived from cytomegalovirus (CMV) was added to the hybridisation reaction at 5 pM concentration. The results showed a significant effect in reducing non-specific binding with the addition of the amine PEG. The particles with PEG treatment gave an average signal of 14 000 ± 2500, while the non-PEG treated particles gave a higher signal of 23 400 ± 2500 ($n = 3$). All subsequent coupling reactions were conducted with the addition of the amine PEG at 3×10^6 molar equivalents to particles and 1×10^{13} probes per cm^2.

Capture probe optimisation on magnetic beads

While the current assay was established and optimised in a monoplex format, the capture probe immobilisation

architecture was designed to enable multiplexing. In this manner a 166 bp linker was ligated with a target specific 39 basepair capture probe with a common ligation sequence and unique probe sequence. The double stranded linker had a number of functions: (a) the negatively charged phosphodiester backbone helped reduce non-specific interactions between the magnetic nanoparticles and the polystyrene reporter particles, (b) the linker also served to increase the number of target molecules which can hybridise between the particles due to its extended length.

Two capture probe immobilisation methods were investigated. Ligation was conducted on or off the bead with the linker to bead concentration modified to be 1.2, 1, 0.8, 0.6 times the biotinylated oligobinding capacity of the beads as stipulated by the supplier. Stoichiometric biotin binding capacity yields a theoretical coupling density of 2.4×10^{12} biotins per cm^2. The results (ESI†, Fig. 3) show that ligation prior to coupling to the beads leads to a stronger signal to noise ratio for the 1.2× and 1× molar excess of linker to biotin capacity of the bead. The 1.2× molar excess showed the least background signal. All future magnetic bead coupling reactions were conducted with ligation prior to coupling the linker to the magnetic nanoparticle with a 1.2× molar ratio of linker to biotin binding capacity.

Hybridisation buffer

According to the well established DVLO (Dergaguin, Verwey, Landau and Overbeek)[39,40] theory, as the ionic strength of the dispersant increases, the Debye double layer length decreases, thereby enabling the short range van der Waals forces to become influential with resultant aggregation of the particles. Non-specific aggregation could have a detrimental effect on the assay as monodisperse particles are required to maintain a high particle loading. In contrast the cations in the hybridisation buffer are required to shield the negative charges of both the immobilised capture and reporter probes and the target DNA to enable their interaction. Therefore it was important to determine experimentally how ionic strength affected the sensitivity of the assay.

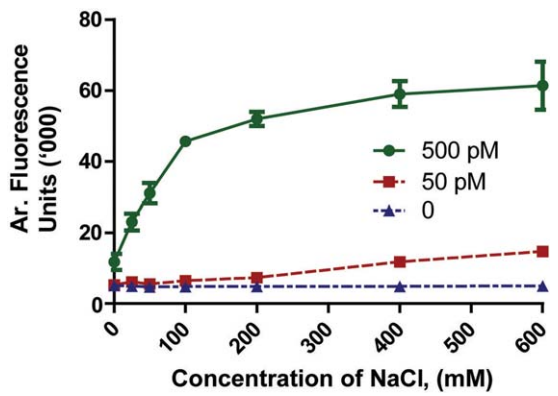

Fig. 5 Aggregate fluorescent signal obtained from hybridisation reactions with 7.3×10^8 fluorescent particles and 10^7 magnetic particles conducted with different salt concentrations. Signal from 500 pM (green circles) target DNA shows strong increase in signal, while no detectable increase in signal for the zero DNA hybridisation reaction was measured (blue triangles). 600 mM is equivalent to 4× SSC. Buffer also trisodium citrate at 1/10 the NaCl concentration.

The results presented in Fig. 5 show that ionic strength up to 600 mM NaCl improved hybridisation yields for the assay, while causing undetectable non-specific pulldown of fluorospheres (blue triangles in Fig. 5). Consequently, 4× SSC (600 mM NaCl, 60 mM trisodium citrate) with 0.1% Triton X-100 was used as the hybridisation buffer for the remainder of the study.

Particle concentration

The number of particles loaded into the reaction was modified to determine the effect of particle concentration on sensitivity. The results (Fig. 6) indicate that increasing the number of magnetic or fluorescent nanoparticles within the reaction doesn't significantly affect the sensitivity as measured with the aggregate fluorescence technique. A key trend observed during the particle loading experiments was that the background signal increased as more beads were added to the reaction. While the results show that sensitivity was in fact dependent on particle loading (Fig. 6), the remainder of the assays reported in this current work was conducted with 1.0×10^7 and 7.3×10^8 magnetic and fluorescent particles, respectively.

Single particle and aggregate counting

Following the establishment of coupling conditions for the magnetic and fluorescent particles, the selection of the surfactant and hybridisation buffer ionic strength, the assay was conducted and analysed in the microfluidic chambers on a confocal microscope. The assay employed a wider dynamic range of target concentrations and used the microfluidic chambers and laser scanning confocal microscope for quantification of fluorescent particles. Following the automated washing steps, the particles were eluted into 30 μL and injected into different chambers within the microfluidic device and subsequently placed on a 50 mm diameter magnet to pull the particles onto the surface of the coverslip. The device was then inspected with a confocal

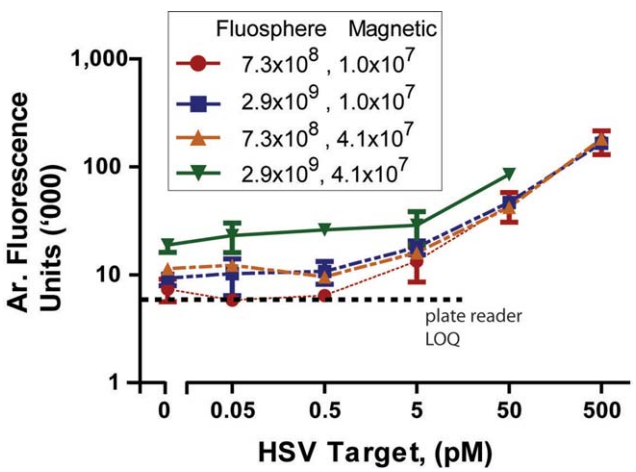

Fig. 6 Effect of nanoparticle concentration on assay sensitivity as determined by an aggregate fluorescent measurement following a 90 μL hybridisation reaction and automated washing steps. Adding four times of either type of particle increased the background signal and sensitivity to the same degree, while increasing both particles by four times increased the background signal further.

microscope with images of the yellow green fluorescent nanoparticles analysed using ImageJ (NIH) to count the particles and aggregates which were then plotted (Fig. 7).

In order to establish the limit of detection, defined as three times the standard deviation of the background, the images for the dose response were analysed. An average of 19.6 counted particles within a 421 × 421 μm^2 field of view (s.d 6.7, $n = 3$) was established yielding a limit of detection of 0.8 pM, which corresponds to 72 attomoles of target DNA. A limit of quantification, based on ten times the standard deviation of the background, of 4 pM (360 attomoles) for the 90 μL initial hybridisation volume.

In order to better understand the sensitivity limits for the assay, we calculated the distribution of target molecules across the magnetic beads and then related this distribution to the number of molecules binding the 200 nm polystyrene nanoparticles to the 500 nm magnetic particles. Taking into account the high ionic strength of the buffer, the near continual mixing and the 90 μL reaction volume, it was assumed that all target molecules hybridised with capture probes within the 90 minute hybridisation reaction. Assuming that 360 attomoles of target DNA were uniformly distributed over the surface of the 10^7 magnetic beads, each particle was coated with ~21 target molecules, with an average area of 3.7 × 10^{-10} cm^2 per target. The following additional assumptions have been made to estimate the number of target molecules linking the magnetic and fluorescent nanoparticles: (a) the 166 bp DNA linker on the magnetic bead surface can stretch to ¾ of its full extended length of 0.34 nm per bp[41] and, therefore, the target DNA immobilised on the linker DNA could hybridise with reporter probes immobilised on the fluosphere approximately 42 nm from the magnetic bead surface; (b) the linker DNA can be compressed to 4.2 nm. This leads to the prediction that the surface area of the two particles which come into contact, allowing DNA molecules to hybridise, equals 1.6 × 10^{-10} cm^2. As a result, and with the assumption that 21 target molecules are distributed uniformly over the magnetic beads with an average area of 3.7 × 10^{-10} cm^2 there are single molecules binding the fluospheres to the magnetic particles.

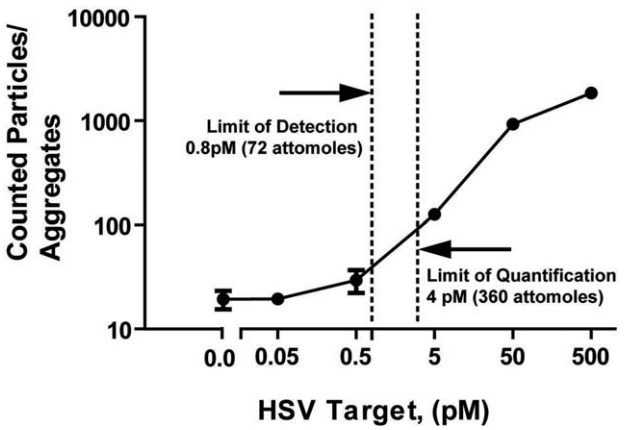

Fig. 7 Assay dose response generated for a synthetic Herpes Simplex Virus DNA molecule. Following hybridisation, the number of fluorescent particles and aggregates from a dose series of target DNA was determined from within microfluidic chambers on the confocal fluorescent microscope. The limit of detection is defined as three times the standard deviation while limit of quantification as ten times the standard deviation of the background.

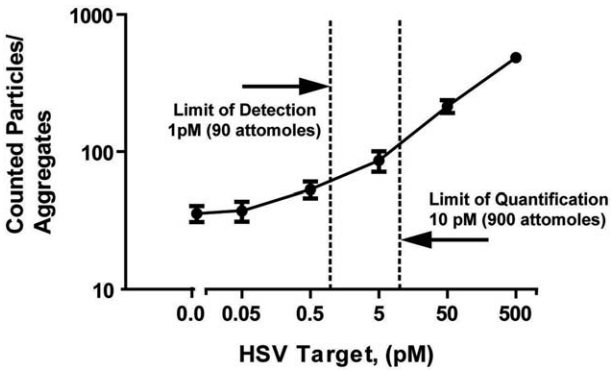

Fig. 8 Number of particles/aggregates counted in an assay with target DNA spiked into swine CSF prior to being added to the hybridisation reaction.

The assay was conducted in swine cerebrospinal fluid (CSF) to test its performance in a biological matrix. The assay was conducted identically to that in hybridisation buffer experiment except that the DNA dose response was generated in swine CSF, as opposed to hybridisation buffer. The results were similar to those obtained for the hybridisation buffer with a limit of detection of 1 pM which correlates with 90 attomoles (Fig. 8).

The nucleic acid detection method reported here demonstrates sensitivity in the low pM (fmol) range with a detection method based on counting individual fluorescent particles and aggregates in a microfluidic chamber. While providing sensitivity superior to a fluorescence plate reader, the hybridisation and counting method is significantly less sensitive than amplification-based detection protocols. For instance, Pandori *et al.*[6] demonstrated a 10 copy detection limit for HSV with a quantitative PCR reaction. Therefore, in order to progress towards clinical utility, the technique reported here requires improved sensitivity, sample throughput and capacity to better pre-concentrate analyte and allow for larger sample volume passage within the microfluidic device. The technique would also benefit from automation as a practical method to analyse a larger number of replicates and samples in a timely manner. Efforts to address these issues are currently underway.

Conclusions

A set of reagents for a magnetic and fluorescent nanoparticle based assay has been optimised. The optimised coupling quantity for an amine terminated reporter probe to carboxylic acid functionalised fluorescent polystyrene particles was 10^{13} reporter probes per cm^2 of particle surface. These particles were subsequently co-modified with an amine terminated polyethylene glycol to reduce non-specific binding. The preferred method for immobilising a capture probe *via* a 166 basepair linker to the streptadivin coated magnetic particle was also investigated. Optimum hybridisation was measured using solution phase ligation of the capture probe followed by coupling using the biotinylated linker. The assay gave a limit of quantification of 4 pM which correlated with single target strands able to bind the fluorescent nanoparticles to the magnetic nanoparticles.

Acknowledgements

DT acknowledges the University of Queensland for his PhD scholarship. The SEM was kindly conducted by Kathryn Green at the Centre for Microscopy and Microanalysis. The microfabrication was conducted at the Queensland node of the Australian National Fabrication Facility. The swine CSF was collected with kind assistance from Cora Lau from the UQ School of Veterinary Science. This work was supported by NHMRC Australia Fellowship AF 511105. Ethics approval for CSF collection was obtained for tissue sharing under UQ AEC project number HMRC/RBH/564/09. The authors thank members of the Cooper group for reviewing the manuscript.

References

1 R. J. Whitley and F. Lakeman, *Clin. Infect. Dis.*, 1995, **20**, 414–420.
2 A. Hjalmarsson, P. Blomqvist and B. Skoldenberg, *Clin. Infect. Dis.*, 2007, **45**, 875–880.
3 R. J. Whitley and J. W. Gnann, *Lancet*, 2002, **359**, 507–513.
4 A. H. Rowley, R. J. Whitley, F. D. Lakeman and S. M. Wolinsky, *Lancet*, 1990, **335**, 440–441.
5 A. Sauerbrei, U. Eichhorn, C. Hottenrott and P. Wutzler, *J. Clin. Virol.*, 2000, **17**, 31–36.
6 M. W. Pandori, J. Lei, E. H. Wong, J. Klausner and S. Liska, *BMC Infect. Dis.*, 2006, **6**, 9.
7 R. J. Whitley and J. W. Gnann, *Clin. Infect. Dis.*, 2007, **45**, 881–882.
8 J. J. Storhoff, A. D. Lucas, V. Garimella, Y. P. Bao and U. R. Muller, *Nat. Biotechnol.*, 2004, **22**, 883–887.
9 J.-M. Nam, S. I. Stoeva and C. A. Mirkin, *J. Am. Chem. Soc.*, 2004, **126**, 5932–5933.
10 P. Huhtinen, J. Vaarno, T. Soukka, T. Lovgren and H. Harma, *Nanotechnology*, 2004, **15**, 1708–1715.
11 J. A. Hansen, R. Mukhopadhyay, J. Ã. Hansen and K. V. Gothelf, *J. Am. Chem. Soc.*, 2006, **128**, 3860–3861.
12 A. Agrawal, R. Deo, G. D. Wang, M. D. Wang and S. M. Nie, *Proc. Natl. Acad. Sci. U. S. A.*, 2008, **105**, 3298–3303.
13 M. Stocher, V. Leb, M. Bozic, H. H. Kessler, G. Halwachs-Baumann, F. Landt, H. Stekel and J. Berg, *J. Clin. Virol.*, 2003, **26**, 85–93.
14 R. Owczarzy, A. V. Tataurov, Y. Wu, J. A. Manthey, K. A. McQuisten, H. G. Almabrazi, K. F. Pedersen, Y. Lin, J. Garretson, N. O. McEntaggart, C. A. Sailor, R. B. Dawson and A. S. Peek, *Nucleic Acids Res.*, 2008, **36**, W163–W169.
15 A. Perrin, T. Martin and A. Theretz, *Bioconjugate Chem.*, 2001, **12**, 678–683.
16 S. Cai, L. Xin, C. W. Lau and J. Z. Lu, *Analyst*, 2010, **135**, 615–620.
17 S. Sam, L. Touahir, J. S. Andresa, P. Allongue, J. N. Chazalviel, A. C. Gouget-Laemmel, C. H. de Villeneuve, A. Moraillon, F. Ozanam, N. Gabouze and S. Djebbar, *Langmuir*, 2010, **26**, 809–814.
18 D. C. Duffy, J. C. McDonald, O. J. A. Schueller and G. M. Whitesides, *Anal. Chem.*, 1998, **70**, 4974–4984.
19 M. D. Abramoff, P. J. Magelhaes and S. J. Ram, "Image Processing with ImageJ", *Biophotonics International*, 2004, **11**(7), 36–42.
20 A. W. Peterson, R. J. Heaton and R. M. Georgiadis, *Nucleic Acids Res.*, 2001, **29**, 5163–5168.
21 T. Springer, H. Sipova, H. Vaisocherova, J. Stepanek and J. Homola, *Nucleic Acids Res.*, 2010, **38**, 7343–7351.
22 R. Levicky and A. Horgan, *Trends Biotechnol.*, 2005, **23**, 143–149.
23 J. N. Kremsky, J. L. Wooters, J. P. Dougherty, R. E. Meyers, M. Collins and E. L. Brown, *Nucleic Acids Res.*, 1987, **15**, 2891–2909.
24 S. F. Wolf, L. Haines, J. Fisch, J. N. Kremsky, J. P. Dougherty and K. Jacobs, *Nucleic Acids Res.*, 1987, **15**, 2911–2926.
25 S. A. Dunbar, *Clin. Chim. Acta*, 2006, **363**, 71–82.
26 P. L. Biancaniello, J. C. Crocker, D. A. Hammer and V. T. Milam, *Langmuir*, 2007, **23**, 2688–2693.
27 A. J. Kim, P. L. Biancaniello and J. C. Crocker, *Langmuir*, 2006, **22**, 1991–2001.
28 A. J. Kim, R. Scarlett, P. L. Biancaniello, T. Sinno and J. C. Crocker, *Nat. Mater.*, 2009, **8**, 52–55.
29 M. P. Valignat, O. Theodoly, J. C. Crocker, W. B. Russel and P. M. Chaikin, *Proc. Natl. Acad. Sci. U. S. A.*, 2005, **102**, 4225–4229.
30 R. L. Stears, R. C. Getts and S. R. Gullans, *Physiol. Genomics*, 2000, **3**, 93–99.
31 B. Huang, H. K. Wu, S. Kim and R. N. Zare, *Lab Chip*, 2005, **5**, 1005–1007.
32 G. T. Hermanson, *Bioconjugate Techniques*, Elsevier Academic Press, Amsterdam, Boston, 2nd edn, 2008.
33 P. Harder, M. Grunze, R. Dahint, G. M. Whitesides and P. E. Laibinis, *J. Phys. Chem. B*, 1998, **102**, 426–436.
34 M. Zheng, F. Davidson and X. Y. Huang, *J. Am. Chem. Soc.*, 2003, **125**, 7790–7791.
35 E. E. Foos, A. W. Snow, M. E. Twigg and M. G. Ancona, *Chem. Mater.*, 2002, **14**, 2401–2408.
36 T. Matsuya, S. Tashiro, N. Hoshino, N. Shibata, Y. Nagasaki and K. Kataoka, *Anal. Chem.*, 2003, **75**, 6124–6132.
37 S. I. Jeon, J. H. Lee, J. D. Andrade and P. G. Degennes, *J. Colloid Interface Sci.*, 1991, **142**, 149–158.
38 A. J. Kim, V. N. Manoharan and J. C. Crocker, *J. Am. Chem. Soc.*, 2005, **127**, 1592–1593.
39 B. V. Derjaguin and L. Landau, *Acta Physicochim. URSS*, 1941, **14**, 633–662.
40 E. F. W. Verwey, and J. Th. G. Overbeek, *Theory of the Stability of Lyophobic Colloids*, Elsevier, Amsterdam, 1948.
41 T. R. Strick, M. N. Dessinges, G. Charvin, N. H. Dekker, J. F. Allemand, D. Bensimon and V. Croquette, *Rep. Prog. Phys.*, 2003, **66**, 1–45.